Molecular and electronic ground and excited structures of heteroleptic ruthenium polypyridyl dyes for nanocrystalline TiO_2 solar cells†

Nobuko Onozawa-Komatsuzaki, Osamu Kitao,* Masatoshi Yanagida, Yuichiro Himeda, Hideki Sugihara and Kazuyuki Kasuga*

Received (in Montpellier, France) 23rd August 2005, Accepted 3rd March 2006
First published as an Advance Article on the web 17th March 2006
DOI: 10.1039/b511986c

Heteroleptic ruthenium complexes of the type *cis*-[Ru(H_2dcbpy)(L)($NCS)_2$], where H_2dcbpy = 4,4′-dicarboxy-2,2′-bipyridine and L = 1,10-phenanthroline (phen) (**1**) or dipyrido[3,2-*a*:2′,3′-*c*]-phenazine (dppz) (**2**), were synthesized and their photochemical properties were investigated. The complexes showed a broad and intense metal-to-ligand charge transfer (MLCT) transition band in the visible region. The complexes were anchored to nanocrystalline TiO_2 film electrodes, and the photovoltaic properties of the resulting dye-sensitized solar cells were characterized and compared with the properties of cells prepared with *cis*-$(NBu_4)_2$[Ru(Hdcbpy)$_2$($NCS)_2$] (**N719**). The efficiency of the **2**-sensitized solar cell was 20% lower than that of the **1**-sensitized solar cell, but neither was as efficient as the **N719**-sensitized solar cell. The electronic structures of the complexes were investigated by means of a time-dependent density functional theory method in an effort to better understand their effectiveness in TiO_2-based photoelectrochemical cells. The calculation results indicated that the character of the MLCT transitions in the long wavelength region differed between **1** and**2**, although their energy levels are nearly the same in the protonated forms. It was suggested that the performance of the **2**-sensitized solar cell could be improved by the introduction of electron-donating groups on the dppz ligand of **2**.

Introduction

Photoelectrochemical systems with dye-sensitized metal oxide semiconductor electrodes have permitted the construction of low-cost photovoltaic devices over the past two decades.[1] O' Regan and Grätzel have developed a highly efficient dye-sensitized solar cell (Grätzel cell)[2] consisting of **N3** dye (*cis*-[Ru(H_2dcbpy)$_2$($NCS)_2$]) (H_2dcbpy = 4,4′-dicarboxy-2,2′-bipyridine) adsorbed on nanocrystalline TiO_2 films. These dyes show remarkably improved light-harvesting efficiency relative to other dyes developed before it,[3] and much effort has been directed toward the development of highly efficient solar cells based on dye sensitization. In such solar cells, the excited state of the dye sensitizer, generated by absorption of light, plays the important role of injecting an electron into the conduction band of the semiconductor.

Octahedral Ru(II) polypyridyl complexes such as **N719** (*cis*-$(NBu_4)_2$[Ru(Hdcbpy)$_2$($NCS)_2$])[4] and black dye (*cis*-[Ru(tcterpy)($NCS)_3$]; tcterpy = 4,4′,4″-tricarboxy-2,2′:6′,2′-terpyridine)[5] are attractive sensitizers because of their favorable light absorption, redox properties, luminescence emission, excited state lifetime and photostability in the devices.[2–8] In dye-sensitized solar cells (DSSCs) containing **N719** and black dye anchored on nanocrystalline TiO_2 films, high efficiencies (up to 10%) have already been achieved;[4,5] however, further performance enhancement is necessary for practical use. Therefore, the development of new types of Ru(II) polypyridyl complexes is being extensively studied. For example, the absorption properties of Ru(II) polypyridyl complexes can be tuned by changing the structures of the main ligand or an auxiliary ligand. By this method, researchers have attempted to extend the absorption band to longer wavelengths to improve the efficiency of the DSSCs.[9–11] Our group[12–14] and other groups[15,16] have developed new types of Ru(II) polypyridyl complexes for this purpose.

Here, we report the synthesis and photoelectrochemical properties of heteroleptic Ru complexes of the type *cis*-[Ru(H_2dcbpy)(L)($NCS)_2$], where H_2dcbpy = 4,4′-dicarboxy-2,2′-bipyridine and L = 1,10-phenanthroline (phen) (**1**) or dipyrido[3,2-*a*:2′,3′-*c*]-phenazine[17] (dppz) (**2**). In these complexes, one of the H_2dcbpy ligands of **N3** has been replaced. Ru complexes having dppz or its derivatives as a ligand have been of much interest because of their unique emission properties arising from extended aromatic structures incorporating a phenazine moiety.[18–23] The photoelectrochemical properties of the Ru complexes having these ligands as sensitizers for DSSCs are attractive because electron π-conjugation over the aromatic moieties allows long-distance, yet strong, electronic interaction between the dppz ligand and the nanocrystalline TiO_2.[24]

National Institute of Advanced Industrial Science and Technology (AIST), Tsukuba Central 5, 1-1-1 Higashi, Tsukuba, Ibaraki 305-8565, Japan. E-mail: k.kasuga@aist.go.jp

† Electronic supplementary information (ESI) available: Tables: energies of frontier MOs for **N3** and deprotonated-**N3**; selected calculated excited states for **N3**, deprotoned-**N3**, **1**, deprotonated-**1**, **2** and deprotonated-**2** *in vacuo* and in CH_3CN. Figures: molecular orbital of **N3**, **1**energy levels of **N3**, **1** and **2** and deprotonated-**N3**, deprotonated-**1** and deprotonated-**2** in *vacuo*; calculated electronic spectra of **N3**, **1** and **2** *in vacuo* and in CH_3CN and deprotonated-**N3**, deprotonated-**1** and deprotonated-**2** *in vacuo*. See DOI: 10.1039/b511986c

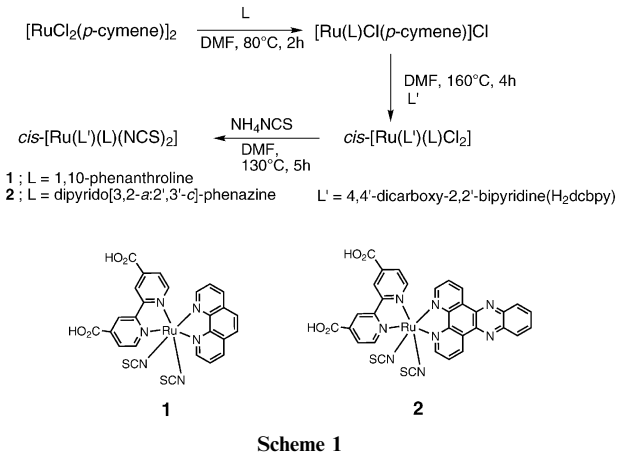

Scheme 1

In this study, we also investigated the electronic structures of these complexes by means of a time-dependent density functional theory (TD-DFT) method in an effort to better understand the effectiveness of these molecules in TiO_2-based photoelectrochemical cells. A detailed understanding of the electronic structure of the excited state of a sensitizer in the visible region is important because the excited state controls the photoelectric conversion efficiency of DSSCs. TD-DFT calculations have proven quite reliable in describing the electronic spectra of complexes containing transition metals, [25–27] also in solution.[28] In the case of Ru complex dyes, many semi-empirical approaches have been reported; however, there have been only a few reports of TD-DFT and *ab initio* studies of **N3** dye,[29–33,34] **N719**,[35] and black dye,[36] *cis*-[Ru(tcterpy)(tripyridine-thiolato)].[37] In this work, we show that with a reasonable computational effort TD-DFT satisfactorily summarizes the spectroscopic properties of the Ru complexes **1** and **2**, suggesting that this approach could be used to provide insight for the design of new and more efficient solar cells sensitizers.

Results and discussion

Synthesis

Heteroleptic ruthenium complexes of the type *cis*-[Ru(H_2dcbpy)(L)(NCS)$_2$], where L = phen or dppz, were synthesized by means of the reported method (Scheme 1).[38] Reaction of [$RuCl_2$(*p*-cymene)]$_2$ in DMF solution at 80 °C with L yielded mononuclear complexes [Ru(L)Cl(*p*-cymene)]Cl. Heteroleptic dichloro complexes [$RuCl_2$(L′)(L)] were prepared from mononuclear complexes [Ru(L)Cl(*p*-cymene)]Cl with L′ (H_2dcbpy) under reduced-light conditions at 160 °C. The *cis*-[Ru(L′)(L)Cl_2] complexes were treated with a 30-fold excess of ammonium thiocyanate to afford *cis*-[Ru(L′)(L)(NCS)$_2$]. ^{1}H NMR spectroscopy indicated that the major products were the *N*-bound isomers, although *S*-bound isomers were also produced as minor products. The complexes were purified as their tetrabutylammonium salts because of solubility problems. The *N*-bound isomers were separated from the *S*-bound ones on a Sephadex LH-20 column with methanol as eluent.

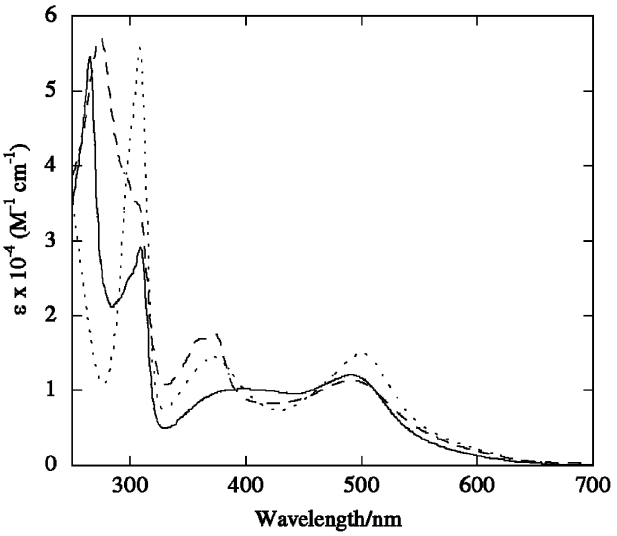

Fig. 1 UV-Vis absorption spectra of **N719** (···), **1** (—), and **2** (--) in 0.01 M aqueous NaOH at room temperature.

Spectroscopic properties

The relevant spectroscopic properties of the complexes and **N719** are summarized in Table 1, and the UV-Vis absorption spectra are shown in Fig. 1. The absorption bands in the 400–700 nm region can be assigned to the MLCT (metal-to-ligand charge transfer) transition bands, as for other Ru(II) polypyridyl complexes.[39,40] The emission maxima of the complexes at 77 K appeared at 694 nm. Both complexes had a 0–0 transition energy (E^{00}) of 1.85 eV, as determined from a tangent to the high-energy side of the corrected emission spectra.[12] This value was almost the same as that of **N719**. The oxidation potentials $E_{1/2}(Ru^{III/II})$ of **1** and **2** in the ground state were +0.80 and +0.83 V, respectively; and the excited-

Table 1 Absorption, luminescence, and electrochemical properties of the sensitizers

	λ_{max}[a]/nm ($\varepsilon/10^3$ M^{-1} cm^{-1})		Emission[b] (77 K)		Electrochemical properties[d] ($E_{1/2}$/V *vs.* SCE)		
Sensitizer	π–π* band	MLCT band	λ_{max}/nm	E^{00} [c]/eV	$Ru^{III/II}$	L/L$^-$ [e]	$Ru^{III/II*}$ [f]
1	267 (57), 309 (29)	400 (sh,10), 492 (12)	694	1.85	+0.80	−0.78	−1.05
2	275 (57), 310 (sh, 35)	374 (18), 492 (11)	694	1.85	+0.83	−0.87	−1.02
N719	219 (59), 309 (56)	372 (14), 500 (15)	702	1.81	+0.78	−0.82	−1.03

[a] Measured in a 0.01 M NaOH aqueous solution. [b] Measured in an ethanol/methanol (4 : 1) glass at 77 K. [c] E^{00} is a tangent to the high-energy side of the corrected emission spectra at 77 K. [d] Measured in a 0.1 M Bu_4NClO_4 acetonitrile solution. [e] Peak potentials. [f] $E_{1/2}$ ($Ru^{III/II*}$) = $E_{1/2}$ ($Ru^{III/II}$) − E^{00}.

Table 2 IR bands (cm^{-1}) of **1** and **2** as solids and adsorbed on nanocrystalline TiO_2

Complex	Form	C–H stretch of NBu_4^+	C–N stretch of NCS	C=O stretch	Symmetric stretch of COO^-	Antisymmetric stretch of COO^-
1	Solid	2961, 2933, 2874	2097	1713	1608	1359
	On TiO_2		2105	1719	1599	1390
2	Solid	2960, 2928, 2873	2097	1718	1607	1355
	On TiO_2		2102	1719	1600	1391

state oxidation potentials $E_{1/2}(Ru^{III/II*})$ of **1** and **2** were estimated as −1.05 and −1.02 V, respectively. Because the redox potential of I^-/I_3^- $> E_{1/2}(I^-/I_3^-)$] and the conduction band edge (E_{cb}) of TiO_2 are 0.30 and −0.80 V (as reported by Myung and Licht.[41] and Liu *et al.*, respectively[42]), the $E_{1/2}$ ($Ru^{III/II*}$) values of **1** and **2** are sufficiently negative compared to the E_{cb} value, and the $E_{1/2}(Ru^{III/II})$ values of **1** and **2** in the ground state are sufficiently positive compared to the redox potential of I^-/I_3^-. These results indicate that the **1**- and **2**-sensitized solar cells can be expected to be as efficient as the **N719**-sensitized cells.

The IR data for the complexes as solids and adsorbed on nanocrystalline TiO_2 are summarized in Table 2. The IR spectra of the solid samples show intense bands at 2097 cm^{-1} ascribed to NCS stretching (*N*-bound form).[4] The IR spectra of **1** and **2** adsorbed on nanocrystalline TiO_2 show the C–N stretching bands of NCS (2105 cm^{-1} for **1** and 2102 cm^{-1} for **2**), the C=O stretching of the protonated carboxyl group (COOH, 1719 cm^{-1}), and the antisymmetric and symmetric stretching of the carboxylate (COO^-, 1599 cm^{-1} for **1** and 1600 cm^{-1} for **2**). The energy difference between the antisymmetric ($\nu_{a,COO}$-) and symmetric ($\nu_{s,COO}$-) stretching frequencies of the carboxyl groups was used to estimate the binding mode of the Ru complexes to the TiO_2 surface.[43,44] The energy differences ($\Delta\nu = \nu_{a,COO^-} - \nu_{s,COO^-}$) for **1** (249 cm^{-1}) and **2** (252 cm^{-1}) on TiO_2 were lower than those for the solid samples (209 cm^{-1}); therefore, **1** and **2** appear to be anchored *via* bidentate or bridging coordination to Ti^{4+} on the TiO_2 surface, as is the case for **N719**.[43,44]

Photovoltaic performance

Photovoltaic performance data for the complexes as sensitizers on nanocrystalline TiO_2 are summarized in Table 3, along with the data for **N719**. The incident photon-to-current conversion (IPCE) spectra of nanocrystalline TiO_2 solar cells sensitized with **1** and **2** are shown in Fig. 2. IPCE is defined as

$$\mathrm{IPCE}(\lambda) = \frac{hc}{q\lambda}\left(\frac{J_{sc}(\lambda)}{I(\lambda)}\right) \times 10^6$$

where I, h, c, q, and λ are the irradiation power (W cm^{-2}), Planck's constant (J s), the speed of light in a vacuum (m s^{-1}), the quantity of charge on the electron (C), and the wavelength (nm), respectively.[3] The **1**- and **2**-sensitized solar cells were effectively photosensitized over a large portion of the solar spectrum from 400 to 900 nm as well as the **N719**-sensitized one.[12] The efficiency of the **2**-sensitized solar cell was 20% lower than that of the **1**-sensitized cell, though the **N719**-sensitized solar cell gave the highest efficiency of the three. The coverages (Γ) of **1** and **2** adsorbed on TiO_2 were 3.2×10^{-7} and 4.3×10^{-7} mol cm^{-2}, respectively (Table 3). On the other hand, the coverage of **N719** adsorbed on TiO_2 was 2.4×10^{-7} mol cm^{-2}. Assuming that each dye molecule occupied an area of 150 $Å^2$,[45] we estimated the coverage of **2** on the TiO_2 surface to be 120%. This value indicates that **2** aggregated on the TiO_2 surface. Ruthenium complexes with large π-conjugated ligands such as dppz are known to aggregate easily by π–π intermolecular interactions.[20] This phenomenon presumably occurs on the TiO_2 surface also. Therefore, the aggregation of **2** on the TiO_2 surface may have prevented the transmission of light and may be one reason for the decrease in cell efficiency.[46]

Table 3 Photovoltaic performance data for **1**-, **2**- and **N719**-sensitized solar cells under AM 1.5 illumination (100 mW cm^{-2})

Sensitizer	$\Gamma^a/10^{-7}$ mol cm^{-2}	$IPCE_{max}$ (%)	J_{sc}/mA cm^{-2}	V_{oc}/V	*ff* [b] (%)	η [b] (%)
1	3.2	74	15.3	0.65	0.67	6.7
2	4.3	54	11.7	0.62	0.73	5.3
N719	2.4	74	16.6	0.73	0.73	8.8

[a] The amount of adsorbed Ru complex was determined by desorbing the complex from the TiO_2 film into a 0.01 M NaOH 1 : 1 (v/v) methanol/water solution and measuring the absorption spectrum. [b] *ff* and η are the fill factor and the overall efficiency, respectively.

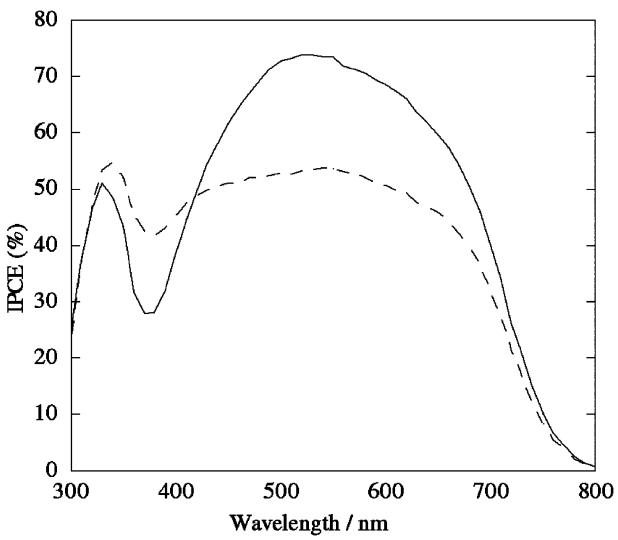

Fig. 2 Photocurrent action spectra for nanocrystalline TiO_2 solar cells sensitized with **1** (—) and **2** (– – –). The incident photon-to-current conversion efficiency (IPCE) is plotted as a function of wavelength.

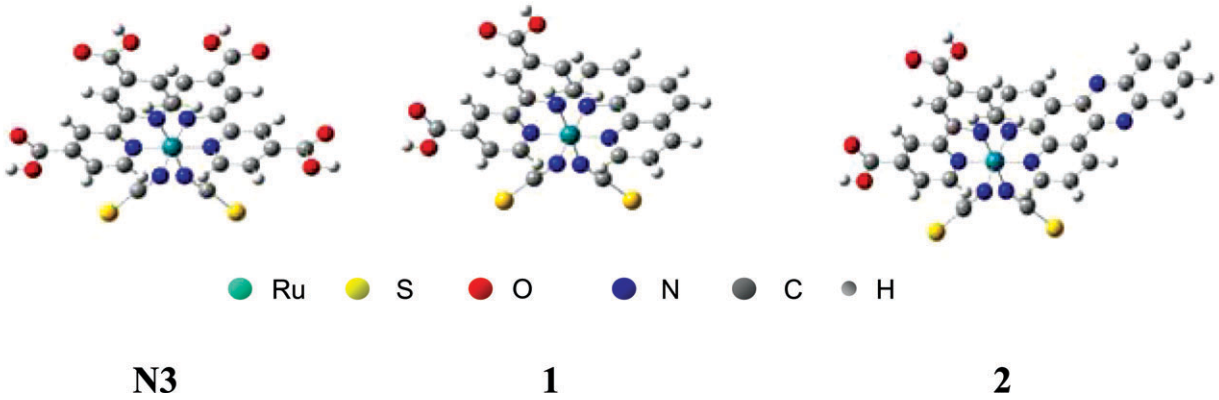

Fig. 3 Optimized molecular structures of Ru(II) polypyridyl complexes **N3**, **1**, and **2** (DFT/B3LYP/CEP-4G).

Electronic structure

The optimized geometries in the singlet ground state of **N3**, **1**, and **2** are illustrated in Fig. 3. The result of **N3** is in agreement with the data reported by Fantacci *et al.*[29] The molecular orbitals (HOMO, LUMO, LUMO + 1) of **1** and **2** are shown in Fig. 4. In the both cases, the electrons on the HOMOs are localized on Ru and on the NCS ligands. In contrast, the electrons on the LUMO and LUMO + 1 of **1** exist on both the dcbpy ligand and the phen ligand, as in the case of **N3** (the molecular orbitals of **N3** are shown in the ESI,† Fig. 1S); whereas the electrons on the LUMO of **2** are localized on the dppz ligand, and those on the LUMO + 1 are localized on the dcbpy ligand.

A detailed analysis of the highest occupied and lowest unoccupied molecular orbitals of **1**, and **2** are presented in Table 4, where orbital energies and dominant moiety contributing to the molecular orbitals are reported. (The data for **N3** are shown in the ESI,† Table 1S.) Since the basis set used for this calculation, CEP-4G, is small, the deprotonated complexes have COO^- based orbitals above the ruthenium based orbitals in the HOMO region.

The energy levels of **N3**, **1**, and **2** (protonated and deprotonated form) in CH_3CN are shown in Fig. 5. (See ESI;† Fig. 2S(a) for the energy levels of **N3**, **1**, and **2** *in vacuo*. Fig. 2S(b) for the those of deprotonated **N3**, **1**, and **2** *in vacuo*.) The energy levels of the protonated forms are nearly the same and this tendency is consistent with the experimental result

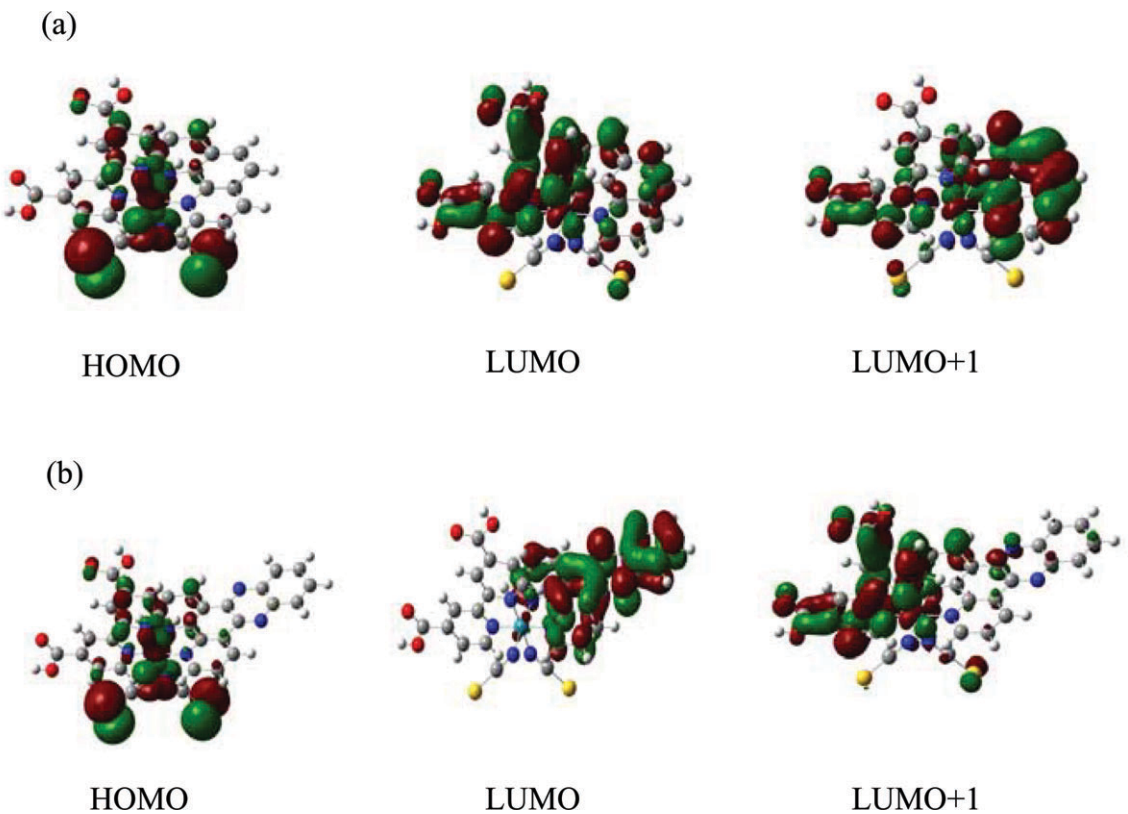

Fig. 4 Molecular orbitals of **1** (a) and **2** (b) (DFT/B3LYP/CEP-4G, isodensity value = 0.02).

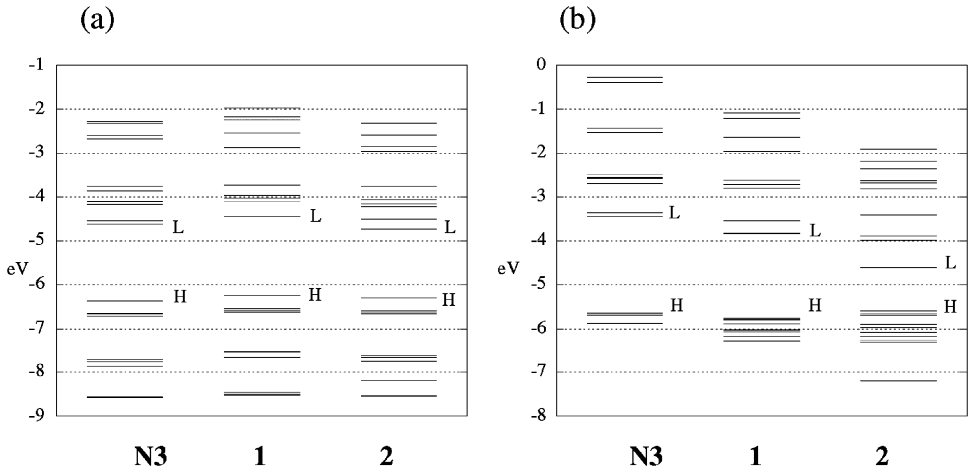

Fig. 5 Energy levels (eV) of **N3**, **1**, and **2** (a) and deprotonated **N3**, **1**, and **2** (b) in CH_3CN. Abbreviations: L, LUMO; H, HOMO.

(Table 1). Deprotonation of the terminal COOH groups substantially destabilizes the occupied and unoccupied orbitals localized on the bipyridine and COO^- moieties.[30] Therefore, the energy levels of the deprotonated form of **N3**, especially those of the LUMOs, are more destabilized than those of deprotonated **1** and **2** because **N3** has four terminal COOH groups whereas the others have only two. Complex **1** is more destabilized than **2** by deprotonation. The molecular size of **1** is smaller than that of **2**; therefore, the effect of destabilization in **1** may be stronger than that in **2**.

TD-DFT calculations of excited states

The absorptions of all of the molecules in the long-wavelength region could be attributed to the MLCT transition. However, as mentioned already among the three dyes, the electronic localization on the LUMO of **2** is unique (Fig. 4(b)). In sensitized solar cells, these dye molecules are adsorbed on nanocrystalline TiO_2 by the carboxylic groups, and electrons are therefore injected into the TiO_2 surface *via* that group.[43,45,47] Electron injection can proceed smoothly in the case of **N3** and **1**, in which the electrons on the LUMO and LUMO + 1 are delocalized. Especially effective electron injection can be expected to occur when the electrons of the LUMO are localized on the dcbpy ligand. In contrast, in the case of **2**, where the electrons of the LUMO exist on the opposite side of the TiO_2 surface, that is, on the dppz ligand, the efficiency of the DSSC may be lower. Because the actual MLCT excited state cannot be described solely in terms of the LUMO, the electronic localization on the dppz ligand for the LUMO in **2** describes only part of the character of the MLCT. However, this localization may be one of the reasons for the lower efficiency of the **2**-sensitized solar cell.

A comparison between the experimental and calculated absorption maxima are summarized in Table 5. The calculated absorption maxima of **N3**, **1** and **2** *in vacuo* and in CH_3CN are similar in value and strength, respectively. On the other hand, those of deprotonated-**N3**, **1** and **2** *in vacuo* and in CH_3CN are a little different among all complexes. The MLCT bands of all the molecules in the lower-energy region are blue-shifted by solvation, and the bands are blue-shifted further by deprotonation. The ligand-based charge transfer (LBCT) transitions of **N3**, which are major in the higher-energy region, are red-shifted by deprotonation; however, those of **1** and **2** are not shifted as much.

The absorption spectra of **N3**, **1**, and **2** under alkaline conditions (Fig. 1) are comparable to the corresponding calculated spectra, which include the effects of solvation and

Table 4 Energies of frontier molecular orbitals obtained from the B3LYP/CEP-4G wavefunction for **1** and **2**

	1			Deprotonated-**1**		
	Energy/eV			Energy/eV		
MO[a]	Type[b]	*In vacuo*	In CH_3CN	Type[b]	*In vacuo*	In CH_3CN
106 (V)	bpy(π*)	−3.82	−3.73	phen(π*)	1.74	−2.71
105 (V)	bpy(π*)	−4.11	−3.97	phen(π*)	1.09	−2.81
104 (V)	phen(π*)	−4.27	−4.02	phen(π*)	0.93	−3.54
103 (V)	phen(π*)	−4.32	−4.12	phen(π*)	0.01	−3.82
102 (V)	bpy(π*)	−4.53	−4.45	phen(π*)	−0.18	−3.84
101 (O)	NCS	−5.77	−6.24	COO^-	−0.51	−5.77
100 (O)	NCS	−5.91	−6.54	COO^-	−0.54	−5.79
99 (O)	Ru(d*)	−6.01	−6.59	COO^-	−0.55	−5.79
98 (O)	Ru(d*)	−6.08	−6.61	COO^-	−0.59	−5.80
97 (O)	Ru(d*)	−7.34	−7.54	COO^-	−0.86	−5.89
	2			Deprotonated-**2**		
	Energy/eV			Energy/eV		
MO[a]	Type[b]	*In vacuo*	In CH_3CN	Type[b]	*In vacuo*	In CH_3CN
124 (V)	bpy(π*)	−4.14	−4.06	dppz(π*)	0.92	−2.82
123 (V)	dppz(π*)	−4.28	−4.16	bpy(π*)	0.82	−3.41
122 (V)	dppz(π*)	−4.33	−4.21	dppz(π*)	0.01	−3.90
121 (V)	bpy(π*)	−4.56	−4.51	dppz(π*)	−0.17	−3.98
120 (V)	dppz(π*)	−4.86	−4.73	dppz(π*)	−0.90	−4.60
119 (O)	Ru(d*)	−5.81	−6.30	COO^-	−1.19	−5.60
118 (O)	NCS	−5.95	−6.60	COO^-	−1.20	−5.67
117 (O)	Ru(d*)	−6.04	−6.63	COO^-	−1.31	−5.70
116 (O)	Ru(d*)	−6.12	−6.67	Ru(d*)	−1.56	−5.90
115 (O)	Ru(d*)	−7.39	−7.62	COO^-	−1.61	−5.98

[a] O: occupied; V: virtual. Bold characters are used for the HOMO (**101** for **1**, and **119** for **2**) and the LUMO (**102** for **1**, and **120** for **2**). [b] Dominant moiety contributing to molecular orbital.

Table 5 Comparison of calculated and experimental values for energies of the absorption maxima

Sensitizer	Solvent	Energies of the absorption maxima/eV				
		Calculated (Oscillator strength/a.u.)			Experimental ($\varepsilon^a/10^4$ M^{-1} cm^{-1})	
N3	*In vacuo*	3.7 (1.1)	2.9 (0.90)	1.5 (0.38)		
	CH_3CN	3.7 (1.8)	3.1 (0.82)	1.9 (0.40)		
Deprotonated-**N3**	*In vacuo*	2.4 (0.11)	1.8(0.18)			
	CH_3CN	2.7 (0.38)	1.9 (0.26)		3.3 (1.4)	2.5 (1.5)
1	*In vacuo*	3.8 (0.73)	2.8 (0.71)	1.5 (0.34)		
	CH_3CN	3.8 (1.0)	3.0 (0.76)	1.9 (0.36)		
Deprotonated-**1**	*In vacuo*	2.7 (0.40)	1.4 (0.19)			
	CH_3CN	2.9 (0.67)	1.9 (0.28)		3.1 (1.0)	2.5 (1.2)
2	*In vacuo*	2.8 (0.86)	1.5 (0.33)			
	CH_3CN	3.8 (2.9)	3.0 (0.98)	1.9 (0.35)		
Deprotonated-**2**	*In vacuo*	2.7 (0.71)	1.5 (0.26)			
	CH_3CN	2.9 (1.4)	2.1 (0.27)		3.3 (1.8)	2.5 (1.1)

[a] Measured in a 0.01 M NaOH aqueous solution.

deprotonation. In Fig. 6, we also compare the experimental spectra of **N3**, **1**, and **2** in alkaline conditions with the electronic spectra of deprotonated **N3**, **1**, and **2** in CH_3CN calculated by the TD-DFT method. Our TD-DFT results with a small basis set does not reproduce the experimental spectra so well as the previous studies with a larger basis set, DGDZVP.[34,35] The differences in the absorption maxima between experimental and calculated spectra are about 0.5 eV among all complexes. Within the investigated energy range, two well separated bands are found with intensity maxima around 3 and 2 eV in all cases. The separation of these two bands, 0.8–1.0 eV is similar with experimental values of 0.6–0.8 eV. Although the absorption edges of all complexes are nearly the same in the MLCT region, the spectra of **1** and **2** are broader than that of **N3**. These results are mostly consistent with the experimental results and may reflect the effect of the disappearance of the symmetry caused by replacing one of the dcbpy ligands of **N3** with the phen or dppz ligand. (All electronic spectra calculated by the TD-DFT method are shown in the ESI†, Fig. 3S–5S.)

As mentioned already, the efficiency (η) of the **2**-sensitized solar cell was lower than that of the **1**-sensitized cell, although both **1** and **2** had similar spectral responses in the visible range (3.1–1.8 eV). From the viewpoint of the molecular orbital levels, this difference can be explained as follows. In the electronic spectra of deprotonated **1** and **2** in the visible range (Fig. 7; see ESI,† Tables 2S–13S, for more-complete data), the contributions of MLCT1 [metal-to-ligand (dcbpy) charge transfer] and MLCT2 [metal-to-ligand (phen) charge transfer] for deprotonated **1** are almost the same in the long-wavelength region; in contrast, for **2**, the contribution of MLCT3 [metal-to-ligand (dppz) charge transfer] is more dominant than that of MLCT1 in the same region. Therefore, to improve the performance of the **2**-sensitized solar cell, introducing electron-donating groups on the dppz ligand and making the contributions of MLCT1 and MLCT3 in the long-wavelength region the same seem to be important. The introduction of electron-donating groups would increase the redox potential of the dppz ligand and is expected to make this ligand difficult to reduce. As a result, most of the electrons would tend to populate the dcbpy ligand, and electron injection into the TiO_2 surface *via* the carboxylic group might proceed more smoothly.

Conclusion

As part of our investigation of efficient sensitizers for DSSCs, we synthesized two new heteroleptic Ru complexes, **1** and **2**. The photochemical properties and efficiencies of DSSCs prepared from these complexes were investigated. The efficiency of the **1**-sensitized solar cell was higher than that of the **2**-sensitized cell, but neither was as efficient as the **N719**-sensitized solar cell. We used the TD-DFT method to study the ground and excited electronic structures of these dyes to better understand the factors that contribute to the effectiveness of these sensitizers for DSSCs. The electronic absorption spectra of the complexes calculated by the TD-DFT method were useful to consider experimental results. By using this method, properties of the molecular orbitals which constitute the electronic state of the complexes, assignment of the excitation spectra and details of features of the excitation state became clear. These calculated results indicate that both **1** and **2** have the same advantages as **N3** in terms of energy levels. On the other hand, it was found that the character of the MLCT transition in the long wavelength region differed between **1** and **2**. It is assumed that this difference affects the efficiency of DSSCs.

Even though the efficiency of the **2**-sensitized solar cell was lower than that of the **1**-sensitized cell, we expect that its performance could be improved by the introduction of electron-donating groups on the dppz ligand.

Experimental

Materials

All synthetic reactions were carried out under a nitrogen atmosphere. All materials were reagent grade and were used as received unless otherwise noted. The dppz ligand was prepared according to a literature procedure.[48] **N719** (*cis*-$(NBu_4)_2$[Ru(Hdcbpy)$_2$(NCS)$_2$]) was purchased from Solaronix S. A. (Lausanne, Switzerland).

Syntheses

***cis*-[Ru(phen)(H$_2$dcbpy)(NCS)$_2$] (1).** [$RuCl_2$(*p*-cymene)]$_2$] (0.122 g, 0.2 mmol) was dissolved in DMF (30 mL), and

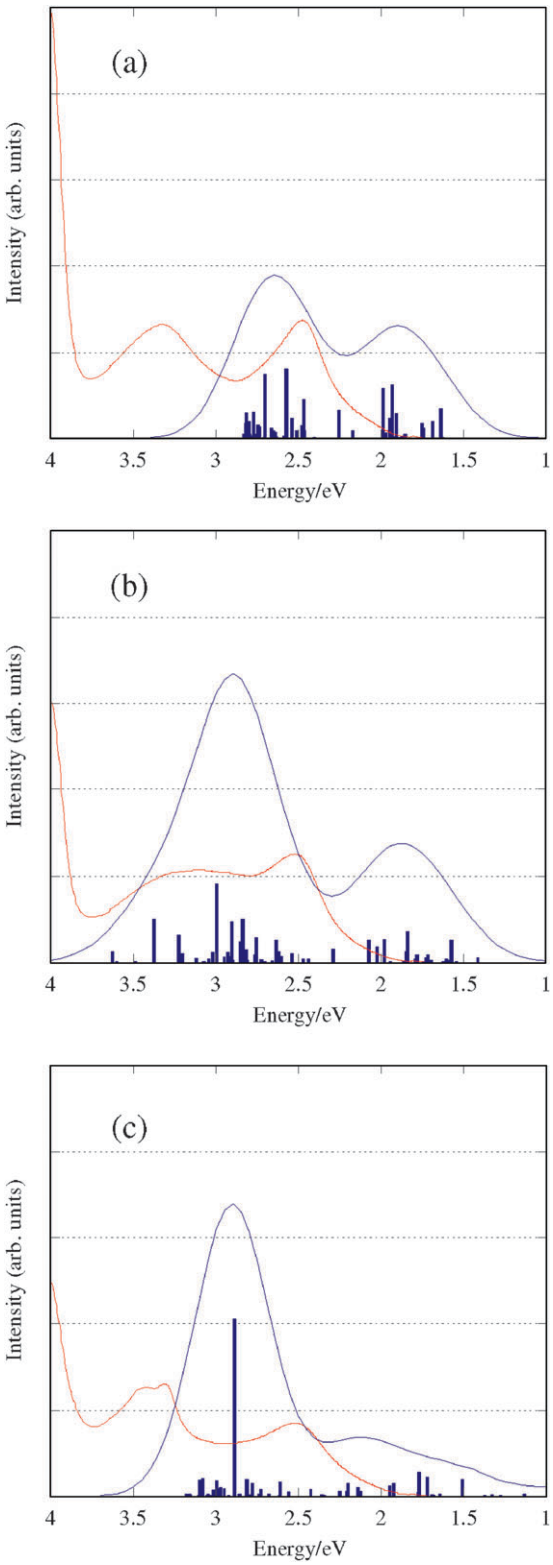

Fig. 6 Comparison between calculated (blue line) and experimental (red lines) spectra of the deprotonated **N3** (a), **1** (b) and **2** (c) in CH_3CN. Blue vertical lines correspond to calculated excitation energies and oscillator strengths. The calculated spectra have been obtained by a gaussian convolution with $\sigma = 0.20$ and 0.1 eV for the transitions below and above 4.0 eV, respectively.

1,10-phenanthroline (0.079 g, 0.4 mmol) was added. The reaction mixture was heated at 80 °C under nitrogen for 2 h, and then 4,4′-dicarboxy-2,2′-bipyridine (0.098 g, 0.4 mmol) was added. The reaction mixture was refluxed at 160 °C for another 4 h under reduced-light conditions to avoid light-induced *cis* to *trans* isomerization. An excess of NH_4NCS (0.99 g, 13 mmol) was then added to the reaction mixture, which was then heated at 130 °C for a further 5 h. The solvent was removed with a rotary evaporator. Water was added to the resulting semi-solid to remove excess NH_4NCS. The water-insoluble product was collected and washed first with distilled water and then with diethyl ether, and dried. The crude complex was dissolved in a solution of tetrabutylammonium hydroxide (0.4 g) in methanol (10 mL). The concentrated solution was charged onto a Sephadex LH-20 column and eluted with methanol. The main red band was collected and concentrated to 3 mL. The required complex was isolated upon addition of a few drops of 0.01 M aqueous HNO_3. The complex was characterized as its tetrabutylammonium (TBA) salt. Yield = 0.29 g (82%). Anal. Calcd (%) for $C_{26}H_{16}N_6O_4S_2Ru \cdot 2H_2O \cdot TBA$: C, 54.88; H, 6.03; N, 10.44. Found: C, 54.40; H, 5.65; N, 10.69%. ESIMS: m/z 882 $(M - H + TBA)^-$. ^1H NMR (400 MHz, CD_3OD) δ 9.75 (dd, J = 5.1, 1.4 Hz, 1H), 9.72 (d, J = 5.9 Hz, 1H), 9.05 (d, J = 1.2 Hz, 1H), 8.87 (d, J = 1.4 Hz, 1H), 8.74 (dd, J = 8.4, 1.2 Hz, 1H), 8.39 (dd, J = 8.4, 1.2 Hz, 1H), 8.30 (dd, J = 5.9, 1.8 Hz, 1H), 8.24 (d, J = 8.8 Hz, 1H), 8.19 (dd, J = 8.2, 5.1 Hz, 1H), 8.12 (d, J = 9.0 Hz, 1H), 7.92 (dd, J = 5.5, 1.2 Hz, 1H), 7.61 (d, J = 6.1, 1H), 7.52 (dd, J = 8.2, 5.3 Hz, 1H), 7.48 (dd, J = 5.9, 1.7 Hz, 1H), 3.23 (t, J = 8.4 Hz, 8H), 1.66 (m, 8H), 1.41 (m, 8H), 1.01 (t, J = 7.3 Hz, 12H).

***cis*-[Ru(dppz)(H_2dcbpy)($NCS)_2$] (2).** Complex **2** was synthesized by the method used for **1** using dppz instead of phen. Yield = 71%. Anal. Calcd (%) for $C_{32}H_{18}N_8O_4S_2Ru \cdot 2H_2O \cdot 0.5TBA$: C, 53.35; H, 4.42; N, 13.22. Found: C, 53.35; H, 4.23; N, 12.93%. ESIMS: m/z 984 $(M - H + TBA)^-$. ^1H NMR (400 MHz, CD_3OD) δ 9.86 (dd, J = 4.1, 1.4 Hz, 1H), 9.67 (d, J = 8.0 Hz, 1H), 9.62 (d, J = 5.7 Hz, 1H), 9.32 (d, J = 8.2 Hz, 1H), 9.06 (s, 1H), 8.88 (s, 1H), 8.38–8.27 (m, 4H), 8.03–7.99 (m, 3H), 7.70 (d, J = 5.9 Hz, 1H), 7.64 (dd, J = 8.1, 5.6 Hz, 1H), 7.45 (dd, J = 5.9, 1.6 Hz, 1H), 3.23 (t, J = 8.3 Hz, 4H), 1.66 (m, 4H), 1.41 (m, 4H), 1.00 (t, J = 7.3 Hz, 6H).

Preparation of dye-sensitized TiO_2 films

Nanocrystalline TiO_2 films were prepared as described in the literature.[8,49–51] The geometric surface area of the TiO_2 film was 0.25 cm^2, and the thickness of the film was 30 μm. The actual inner surface of the TiO_2 film was estimated by BET (Brunauer–Emmett–Teller) measurements. The specific surface area of the nanocrystalline TiO_2 films was estimated to be 57 $m^2\ g^{-1}$. The density of the films (1.8 g cm^{-3}) was calculated by measuring their weight (0.25 $cm^2 \times$ 30 μm). The roughness factor of the films (30 μm) was calculated to be 1970. The thickness of the films was measured with a Tencor Alpha Step 500 profiler. The bare TiO_2 films were dipped in methanolic dye solution at a concentration of 3×10^{-4} M in the presence of 20 mM deoxycolic acid as a co-adsorbent at

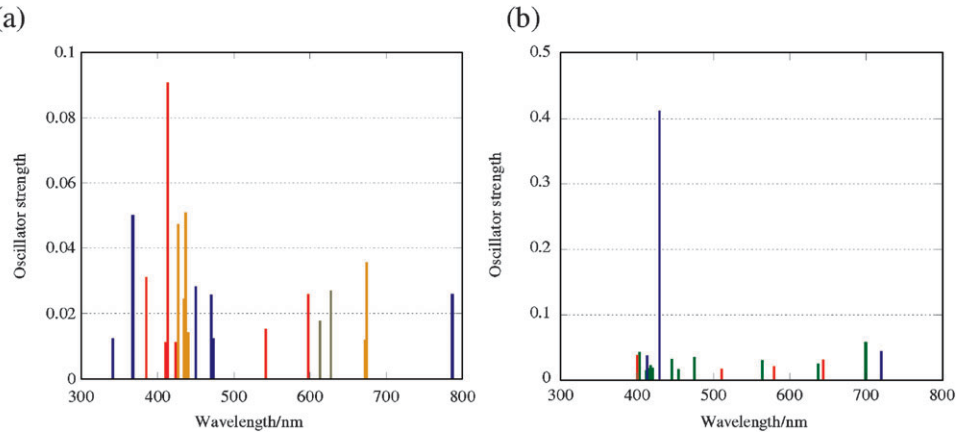

Fig. 7 Calculated electronic spectra in the visible region: (a) deprotonated **1** in CH_3CN and (b) deprotonated **2** in CH_3CN. Blue lines: LBCT (ligand-based charge transfer). Red lines: MLCT1 [metal-to-ligand (bpy) charge transfer]. Orange lines: MLCT2, [metal-to-ligand (phen) charge transfer]. Green lines: MLCT3, [metal-to-ligand (dppz) charge transfer]. Gray lines: [MLCT1 + MLCT2].

room temperature for 20 h. The amount of adsorbed Ru complex (M_{ad}/mol) was determined by desorbing the complex from the TiO_2 film into a 0.01 M NaOH 1 : 1 (v/v) methanol/water solution and measuring the absorption spectrum of the complex. The coverage (Γ) (mol cm^{-2}) is defined as $\Gamma = M_{ad}/0.25$.

Methods

^1H NMR spectra were recorded on a Varian INOVA 400 spectrometer, using tetramethylsilane (TMS) as an internal standard. ESI-MS were measured with a Micromass QUATTRO II mass spectrometer. Elemental analyses were carried out with an Eager 200 instrument. UV-Vis absorption spectra were measured with a Jasco V-550 spectrometer. Corrected emission spectra were obtained with a Hitachi F-4500 spectrofluorimeter. Spectra at 77 K were measured in 4 : 1 (v/v) ethanol/methanol glasses immersed in liquid N_2. All samples for emission measurements were purged with a N_2 stream. IR spectra were measured with a Spectrum One (PerkinElmer) spectrometer with an attenuated total reflectance accessory (ZnSe prism) at a resolution of 4 cm^{-1}. The IR spectra of dyes adsorbed on TiO_2 were corrected for bare TiO_2.

Cyclic voltammetric measurements were performed with an ALS606 instrument in CH_3CN with 0.10 M tetrabutylammonium perchlorate as a supporting electrolyte, and the solution was bubbled with a pure N_2 gas. A three-electrode system was used: a glassy carbon electrode as the working electrode, a Pt wire as the counter electrode, and a Ag/Ag^+ electrode (BAS Co.) as the reference electrode. Ferrocene was used as an internal reference. Cyclic voltammograms, with a scan rate of 100 mV s−1, were evaluated graphically. The concentrations of all sample solutions were kept at 1.0 mM.

Photoelectrochemical measurements were performed in a sandwich-type two-electrode cell consisting of a dye-coated TiO_2 film electrode, a polyethylene film spacer, an electrolyte solution, and a Pt film counter electrode. The electrolyte solution of the cell consisted of 0.6 M (1,2-dimethyl-3-propyl) imidazolium iodide, 0.05 M I_2, and 0.1 M LiI in CH_3CN. The concentration of I_3^- in the electrolyte solution was determined to be 49 mM from the UV-Vis spectrum. The photovoltaic measurements were conducted with a Xe lamp light source simulating the AM 1.5 spectrum (Wacom, WXS-80C-3, 100 mW cm^{-2}). The incident monochromatic photon-to-current conversion efficiency (IPCE) spectra were measured with a monochromatic Xe lamp (SX150C) source (CED99-W, Bunko Keisoku Co.).

Computational methods

All the calculations reported in this paper were performed with the Gaussian 03 program package.[52] Geometry optimizations were carried out, without any symmetry constraints, using the CEP-4G[53–55] basis set. The B3LYP exchange correlation functional[56] was used for all the calculations. TD-DFT[57] excitation energies were computed both *in vacuo* and in solution; calculations in solution were performed using the polarizable continuum model (PCM).[58] The 40 lowest spin-allowed singlet–singlet transitions were taken into account.

Acknowledgements

This work was supported in part by New Energy and Industrial Technology Development Organization (NEDO) under the Ministry of Economy, Trade, and Industry (METI).

References

1 H. Tsubomura, M. Matsumura, Y. Nomura and T. Amamiya, *Nature (London)*, 1976, **261**, 402.
2 B. O'Regan and M. Grätzel, *Nature (London)*, 1991, **353**, 737.
3 M. K. Nazeeruddin, A. Kay, I. Rodicio, R. Humphry-Baker, E. Müller, P. Liska, N. Vlachopoulos and M. Grätzel, *J. Am. Chem. Soc.*, 1993, **115**, 6382.
4 M. K. Nazeeruddin, S. M. Zakeeruddin, R. Humphry-Baker, M. Jirousek, P. Liska, N. Vlachopoulos, V. Shklover, C.-H. Fischer and M. Grätzel, *Inorg. Chem.*, 1999, **38**, 6298.
5 M. K. Nazeeruddin, P. Péchy, T. Renouard, S. M. Zakeeruddin, R. Humphry-Baker, P. Comte, P. Liska, L. Cevey, E. Costa, V. Shklover, L. Spiccia, G. B. Deacon, C. A. Bignozzi and M. Grätzel, *J. Am. Chem. Soc.*, 2001, **123**, 1613.
6 R. Argazzi, C. A. Bignozzi, G. M. Hasselmann and G. J. Mayer, *Inorg. Chem.*, 1998, **37**, 4533.

7 M. Yanagida, L. P. Singh, K. Sayama, K. Hara, R. Katoh, A. Islam, H. Sugihara, H. Arakawa, M. K. Nazeeruddin and M. Grätzel, *J. Chem. Soc., Dalton Trans*., 2000, 2817.
8 K. Sayama, H. Sugihara and H. Arakawa, *Chem. Mater*., 1998, **10**, 3825.
9 M. K. Nazeeruddin, E. Muller, R. Humphry-Baker, N. Vlachopoulos and M. Grätzel, *J. Chem. Soc., Dalton Trans*., 1997, 4571.
10 S. Ruile, O. Kohle, P. Péchy and M. Grätzel, *Inorg. Chim. Acta*, 1997, **261**, 129.
11 S. Ruile, O. Kohle, H. Pettersson and M. Grätzel, *New J. Chem*., 1998, **22**, 25.
12 M. Yanagida, T. Yamaguchi, M. Kurashige, K. Hara, R. Katoh, H. Sugihara and H. Arakawa, *Inorg. Chem*., 2003, **42**, 7921.
13 A. Islam, H. Sugihara, M. Yanagida, K. Hara, G. Fujihashi, Y. Tachibana, R. Katoh, S. Murata and H. Arakawa, *New J. Chem*., 2002, **26**, 966.
14 T. Yamaguchi, M. Yanagida, R. Katoh, H. Sugihara and H. Arakawa, *Chem. Lett*., 2004, **33**, 986.
15 P. Wang, R. Humphry-Baker, J. E. Moser, S. M. Zakeeruddin and M. Grätzel, *Chem. Mater*., 2004, **16**, 3246.
16 C. Klein, M. K. Nazeeruddin, D. Di Censo, P. Liska and M. Grätzel, *Inorg. Chem*., 2004, **43**, 4216.
17 J. E. Dickeson and L. A. Summers, *Aust. J. Chem*., 1970, **23**, 1023.
18 E. Amouyal, A. Homsi, J.-C. Chambron and J.-P. Sauvage, *J. Chem. Soc., Dalton Trans*., 1990, 1841.
19 J.-C. Chambron, J.-P. Sauvage, E. Amouyal and P. Koffi, *Nouv. J. Chim*., 1985, **9**, 527.
20 J. Bolger, A. Gourdon, E. Ishow and J.-P. Launay, *Inorg. Chem*., 1996, **35**, 2937.
21 E. J. Olson, D. Hu, A. Hörmann, A. M. Jonkman, M. R. Arkin, E. D. A. Stemp, J. K. Barton and P. F. Barbara, *J. Am. Chem. Soc*., 1997, **119**, 11458.
22 R. B. Nair, B. M. Cullun and C. J. Murphy, *Inorg. Chem*., 1997, **36**, 962.
23 R. M. Hartshorn and J. K. Barton, *J. Am. Chem. Soc*., 1992, **114**, 5919.
24 B. Gholamkhass, K. Koike, N. Negishi, H. Hori and K. Takeuchi, *Inorg. Chem*., 2001, **40**, 756.
25 A. Rosa, G. Ricciardi, E. J. Baerends and S. J. A. van Gisbergen, *J. Phys. Chem. A*, 2001, **105**, 3311.
26 G. Ricciardi, A. Rosa, S. J. A. van Gisbergen and E. J. Baerends, *J. Phys. Chem. A*, 2000, **104**, 635.
27 A. Rosa, E. J. Baerends, S. J. A. van Gisberge, E. van Lenthe, J. A. Groeneveld and J. G. Snijiders, *J. Am. Chem. Soc*., 1999, **121**, 10356.
28 V. Barone, F. F. de Biani, E. Ruiz and B. Sieklucka, *J. Am. Chem. Soc*., 2001, **123**, 10742.
29 S. Fantacci, F. De Angelis and A. Selloni, *J. Am. Chem. Soc*., 2003, **125**, 4381.
30 F. De Angelis, S. Fantacci and A. Selloni, *Chem. Phys. Lett*., 2004, **389**, 204.
31 O. Kitao, *Proceedings of the 27th Symposium on Chemical Information and Computer Sciences, Tsukuba, Japan*, The Chemical Society of Japan, Division of Chemical Information and Computational Sciences, Japan, 2004, J12, p. 37; http://www.jstage.jst.go.jp/article/ciqs/2004/0/2004_J12/_article.
32 M. Sugimoto, personal communication.
33 J. E. Monat, J. H. Rodriguez and J. K. McCusker, *J. Phys. Chem. A*, 2002, **106**, 7399.
34 F. De Angelis, S. Fantacci and A. Selloni, *Chem. Phys. Lett*., 2005, **415**, 115.
35 M. K. Nazeeruddin, F. De Angelis, S. Fantacci, A. Selloni, G. Viscardi, P. Liska, S. Ito, B. Takeru and M. Grätzel, *J. Am. Chem. Soc*., 2005, **127**, 16835.
36 F. Aiga and T. Tada, *J. Mol. Struct*., 2003, **658**, 24.
37 F. Aiga and T. Tada, *Sol. Energy Mater. Sol. Cells*, 2005, **85**, 437.
38 N. Hirata, J.-J. Lagref, E. J. Palomares, J. R. Durrant, M. K. Nazeeruddin, M. Grätzel and D. Di Censo, *Chem. Eur. J*., 2004, **10**, 595.
39 W. R. McWhinnie and J. D. Miller, *Adv. Inorg. Chem. Radiochem*., 1969, **12**, 135.
40 A. Juris, V. Balzani, F. Barigelletti, S. Campagna, P. Belser and A. von Zelewsky, *Coord. Chem. Rev*., 1988, **84**, 85.
41 N. Myung and S. Licht, *J. Electrochem. Soc*., 1995, **142**, L129.
42 G. Liu, W. Jaegermann, J. He, V. Sundström and L. Sun, *J. Phys. Chem. B*, 2002, **106**, 5814.
43 K. S. Finnie, J. R. Bartlett and J. L. Woolfrey, *Langmuir*, 1998, **14**, 2744.
44 C. Bauer, G. Boschloo, E. Mukhtar and A. Hagfeldt, *J. Phys. Chem. B*, 2002, **106**, 12693.
45 V. Shklover, Yu. E. Ovchinnikov, L. S. Braginsky, S. M. Zakeeruddin and M. Grätzel, *Chem. Mater*., 1998, **10**, 2533.
46 M. Yanagida, T. Yamaguchi, M. Kurashige, G. Fujihashi, K. Hara, R. Katoh, H. Sugihara and H. Arakawa, *Inorg. Chim. Acta*, 2003, **351**, 283.
47 V. Shklover, M. K. Nazeeruddin, S. M. Zakeeruddin, C. Barbé, A. Kay, T. Haibach, W. Steurer, R. Hermann, H.-U. Nissen and M. Grätzel, *Chem. Mater*., 1997, **9**, 430.
48 M. Yamada, Y. Tanaka, Y. Yoshimoto, S. Kuroda and I. Shimao, *Bull. Chem. Soc. Jpn*., 1992, **65**, 1006.
49 K. Hara, H. Sugihara, Y. Tachibana, A. Islam, M. Yanagida, K. Sayama and H. Arakawa, *Langmuir*, 2001, **17**, 5992.
50 K. Hara, H. Horiuchi, R. Katoh, L. P. Singh, H. Sugihara, K. Sayama, S. Murata, M. Tachiya and H. Arakawa, *J. Phys. Chem. B*, 2002, **106**, 374.
51 S. D. Burnside, V. Shklover, Christophe Barbé, P. Comte, F. Arendse, K. Brooks and M. Grätzel, *Chem. Mater*., 1998, **10**, 2419.
52 M. J. Frisch, G. W. Trucks, H. B. Schlegel, G. E. Scuseria, M. A. Robb, J. R. Cheeseman, J. A. Montgomery, Jr, T. Vreven, K. N. Kudin, J. C. Burant, J. M. Millam, S. S. Iyengar, J. Tomasi, V. Barone, B. Mennucci, M. Cossi, G. Scalmani, N. Rega, G. A. Petersson, H. Nakatsuji, M. Hada, M. Ehara, K. Toyota, R. Fukuda, J. Hasegawa, M. Ishida, T. Nakajima, Y. Honda, O. Kitao, H. Nakai, M. Klene, X. Li, J. E. Knox, H. P. Hratchian, J. B. Cross, C. Adamo, J. Jaramillo, R. Gomperts, R. E. Stratmann, O. Yazyev, A. J. Austin, R. Cammi, C. Pomelli, J. W. Ochterski, P. Y. Ayala, K. Morokuma, G. A. Voth, P. Salvador, J. J. Dannenberg, V. G. Zakrzewski, S. Dapprich, A. D. Daniels, M. C. Strain, O. Farkas, D. K. Malick, A. D. Rabuck, K. Raghavachari, J. B. Foresman, J. V. Ortiz, Q. Cui, A. G. Baboul, S. Clifford, J. Cioslowski, B. B. Stefanov, G. Liu, A. Liashenko, P. Piskorz, I. Komaromi, R. L. Martin, D. J. Fox, T. Keith, M. A. Al-Laham, C. Y. Peng, A. Nanayakkara, M. Challacombe, P. M. W. Gill, B. Johnson, W. Chen, M. W. Wong, C. Gonzalez and J. A. Pople, *GAUSSIAN 03 (RevisionA.1)*, Gaussian Inc., Pittsburgh, PA, 2003.
53 W. Stevens, H. Basch and J. Krauss, *J. Chem. Phys*., 1984, **81**, 6026.
54 W. J. Stevens, M. Krauss, H. Basch and P. G. Jasien, *Can. J. Chem*., 1992, **70**, 612.
55 T. R. Cundari and W. J. Stevens, *J. Chem. Phys*., 1993, **98**, 5555.
56 A. D. Becke, *J. Chem. Phys*., 1993, **98**, 5648.
57 R. E. Stratmann, G. E. Scuseria and M. J. Frisch, *J. Chem. Phys*., 1998, **109**, 8218.
58 S. Miertus, E. Scrocco and J. Tomasi, *Chem. Phys*., 1981, **55**, 117.